Data-Driven Control for Radiative Collapse Avoidance in Large Helical Device*)

Tatsuya YOKOYAMA[1,2], Hiroshi YAMADA[1], Suguru MASUZAKI[3,4,5], Byron J. PETERSON[3,4], Ryuichi SAKAMOTO[1,3], Motoshi GOTO[3,4], Tetsutaro OISHI[3,4], Gakushi KAWAMURA[3,4], Masahiro KOBAYASHI[3,4], Toru I TSUJIMURA[3], Yoshinori MIZUNO[3], Junichi MIYAZAWA[3,4], Kiyofumi MUKAI[3,4], Naoki TAMURA[3,4], Gen MOTOJIMA[3,4] and Katsumi IDA[3,4]

[1]*Graduate School of Frontier Sciences, The University of Tokyo, Chiba 277-8561, Japan*
[2]*Research Fellow of Japan Society for the Promotion of Science, Tokyo 102-0083, Japan*
[3]*National Institute for Fusion Science, National Institutes of Natural Sciences, Gifu 509-5292, Japan*
[4]*The Graduate University for Advanced Studies, SOKENDAI, Gifu 509-5292, Japan*
[5]*Advanced Fusion Research Center, Research Institute for Applied Mechanics, Kyushu University, Fukuoka 816-8580, Japan*

(Received 13 December 2021 / Accepted 6 March 2022)

A radiative collapse predictor has been developed using a machine-learning model with high-density plasma experiments in the Large Helical Device (LHD). The model is based on the collapse likelihood, which is quantified by the parameters selected by the sparse modeling, including $\bar{n}_e$, CIV, OV, and $T_{e,edge}$. The control system implementing this model has been constructed with a single-board computer to apply this predictor model to the LHD experiment. The controller calculates the collapse likelihood and regulates gas-puff fueling and boosts electron cyclotron resonance heating in real-time. In density ramp-up experiments with hydrogen plasma, high-density plasma has been maintained by the control system while avoiding radiative collapse. This result has shown that the predictor based on the collapse likelihood has the capability to predict a radiative collapse in real-time.

Keywords: Large Helical Device (LHD), radiative collapse, density limit, stellarator-heliotron plasmas, sparse modeling, data-driven science, plasma control, collapse avoidance

DOI: 10.1585/pfr.17.2402042

1. Introduction

The sudden termination of plasma is a critical risk of a fusion reactor. The most known phenomenon is disruption, which is the major collapse in tokamak plasma. In stellarator-heliotron plasma, where no disruption occurs since the plasma current is not required to sustain the plasma, radiative collapse is the major cause of plasma termination in a high-density regime. The operational density is limited by radiative collapse. Improvement of density limit is an essential issue in fusion energy development because of the advantages of high-density operation for improving confinement for mitigating the divertor heat load. The best-known density limit is the Sudo density [1].

$$n_e^{\mathrm{Sudo}}[10^{20}\mathrm{m}^{-3}] = 0.25 P^{0.5} B^{0.5} a^{-1} R^{-0.5}. \quad (1)$$

Here, P is the absorbed heating power (MW), B is the magnetic field strength on the plasma axis (T), a is the average minor radius (m), and R is the major radius (m).

The data-driven approach using machine learning techniques as recently attracted significant attention in the study of disruption prediction, which is a critical phenomenon in a tokamak [2–5]. Some of these data-driven studies have been applied to the real-time prediction of disruptions in tokamak devices [6, 7].

In our previous studies [8, 9], the collapse likelihood, which shows the probability of the occurrence of radiative collapse, was estimated based on experiment data in Large Helical Device (LHD) [10]. To estimate the likelihood, a linear support vector machine (SVM) [11] was trained with the plasma parameters selected by exhaustive search (ES) [12]. A linear SVM, which is a supervised machine learning technique, was employed as a basic two-class classifier to distinguish "close-to-collapse" discharge data from "stable" data. In the ES, all possible combinations of parameters were evaluated and compared with each other by F1 score [13], which is one of the metrics commonly used in classification problems. The ES is one of the sparse modeling techniques. Sparse modeling is one of the frameworks of data-driven science and it exploits the inherent sparseness in all high-dimensional data to extract the essence of the data [14]. As a result of ES, a combination of key four parameters, $\bar{n}_e$, CIV, OV, and $T_{e,edge}$, has been selected from 15 candidate parameters (see Table 1

author's e-mail: yokoyama.tatsuya17@ae.k.u-tokyo.ac.jp
*) This article is based on the presentation at the 30th International Toki Conference on Plasma and Fusion Research (ITC30).

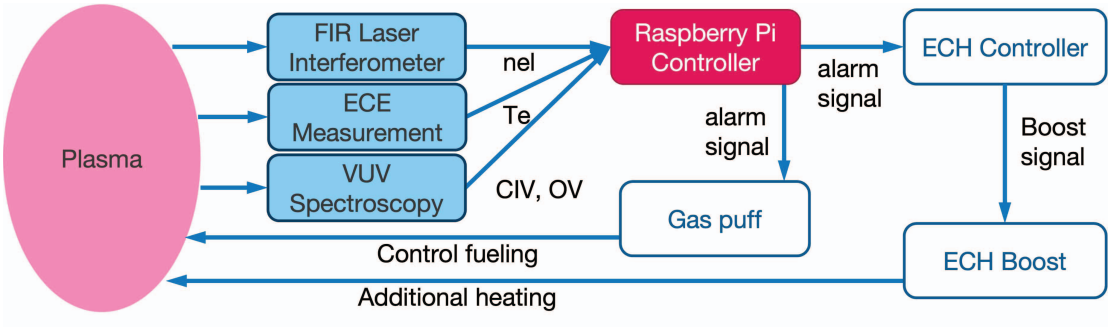

Fig. 1 Schematic diagram of the collapse avoidance control system.

in [9]). Moreover, the proximity of radiative collapse was quantitatively estimated as the "collapse likelihood" using these four key parameters.

In this study, a predictor model of radiative collapse based on the collapse likelihood has been applied to control fueling and heating the LHD plasma to avoid radiative collapse. The remainder of this paper is organized as follows. In section 2, the experimental setup of collapse avoidance is described. The result and discussions of collapse avoidance experiments are presented in section 3. Finally, section 4 presents the conclusion.

2. Development of a Collapse Avoidance Control System

The predictor model based on the collapse likelihood has been applied to a real-time feedback control system for the operation of the LHD. The collapse likelihood was quantitatively evaluated to take the continuous value from zero to one using the key parameters extracted by the ES [8]. Figure 1 shows a schematic diagram of the control system. A single-board computer, Raspberry Pi 4 Model B, with quad-core CPU, 8 GB RAM, and general-purpose input/output (GPIO) interface, has been used as a controller[1]. Since Raspberry Pi does not have any analog input/output interfaces, an analog-digital converter with 24-bit resolution[2] has been used to convert an input analog signal into a digital signal. The controller calculates the collapse likelihood based on the input signals and compares the likelihood with the threshold value, which is given by the GUI interface, in real-time. On average, the controller calculates the likelihood every 8 ms, which is limited by the transmission speed of the Raspberry Pi. When the likelihood exceeds the threshold, an alarm signal is sent out. The alarm signal is turned off when the likelihood falls below the threshold.

When the alarm signal is sent from the controller, the gas-puff control system turns off the fueling and additional power is injected by the electron cyclotron heating (ECH). According to the result of ES-SVM, reducing plasma density and raising edge temperature will effectively reduce the likelihood, i.e., to prevent the occurrence of collapse [8]. Therefore, gas-puff fueling and ECH have been employed as actuators of the control system. The gas puff is one of the main fueling sources in LHD [15]. As ECH, 77 GHz gyrotrons for the fundamental O-mode heating and 154 GHz for the second-harmonic X-mode heating are available. These are controlled by a real-time interlock system [16, 17]. Note that the time duration where ECH can be turned on is limited by its technical capability and the interlock system to avoid a blank injection.

The signals of plasma parameters selected by the feature extraction are input to the controller, i.e., $\bar{n}_e$, CIV, OV, and T_e. As T_e, $T_{e,edge}$ measured using the Thomson scattering measurement has been used in the dataset. However, its time resolution is 30 Hz, which is lower than the requirement of the control system. Therefore, $T_{e,edge}$ has been replaced by $T_{e,ECE}$, which is obtained through the electron cyclotron emission (ECE) measurement with the channel that detects 146.5 GHz. The $T_{e,ECE}$ corresponds to the electron temperature near the center of the plasma, and is only available in experiments with B_t =2.75 T. Here the change in the parameter requires the recalculation of the decision function and the collapse likelihood. The SVM has been trained again with $\bar{n}_e$, CIV, OV, and $T_{e,ECE}$ using available data in the training dataset. The decision function and the collapse likelihood for the control system, $f_{ctrl}(\boldsymbol{x})$ and $\mathrm{Likelihood}_{ctrl}$, are calculated as follows:

$$f_{ctrl}(\boldsymbol{x}) = \exp(2.10)\bar{n}_e^{-0.600}\mathrm{CIV}^{1.31}\mathrm{OV}^{-0.129}T_{e,ECE}^{-1.89}, \tag{2}$$

$$\mathrm{Likelihood}_{ctrl} = \frac{1}{1+\exp\{-14.9\,(\log_{10} f_{ctrl}(\boldsymbol{x}) + 0.283)\}}. \tag{3}$$

The performance of $\mathrm{Likelihood}_{ctrl}$ has not changed significantly from the result of the previous study [8]. In the discharge with control described below (#168701), the $\mathrm{Likelihood}_{ctrl}$ first reached the threshold 11 ms later than the original likelihood. This delay is smaller enough than the averaged prediction margin of 90 ms.

[1] https://www.raspberrypi.org/products/raspberry-pi-4-model-b/
[2] lhttps://www.seeedstudio.com/Raspberry-Pi-High-Precision-AD-DA-Board.html

3. Collapse Avoidance in LHD

3.1 Collapse avoidance experiments

The collapse avoidance with the control system has been attempted in density ramp-up experiments in LHD. Figure 2 shows two typical discharges in hydrogen plasma, with and without collapse avoidance control. In these discharges, the plasma has been sustained by gas-puff fueling and NBI heating. ECH has been used to initiate plasma, while two 154 GHz gyrotrons have been reserved for boost injection.

In the discharge without control, shown by the dashed blue line, a radiative collapse occurred in the early phase of the density ramp-up at around 3.6 s. In this case, the gas puff was injected at a constant until a preset time (about 4.5 s).

On the other hand, in the discharge with control, shown by the solid red line, the radiative collapse in the early phase was successfully avoided by turning gas puff off and boosting ECH. In this case, likelihood threshold has been set as 0.9, shown by the dashed horizontal line in the top panel of Fig. 2. The change in the plasma toward the collapse in the early ramp-up phase was detected about 65 ms before its occurrence, which is earlier enough for a margin of 30 ms for the control. In the discharge with control, the gas puff was turned off within 10 ms after the controller detected the collapse. Meanwhile, the boost ECH was injected about 20 ms later when the controller detected the collapse, while it was earlier than the collapse.

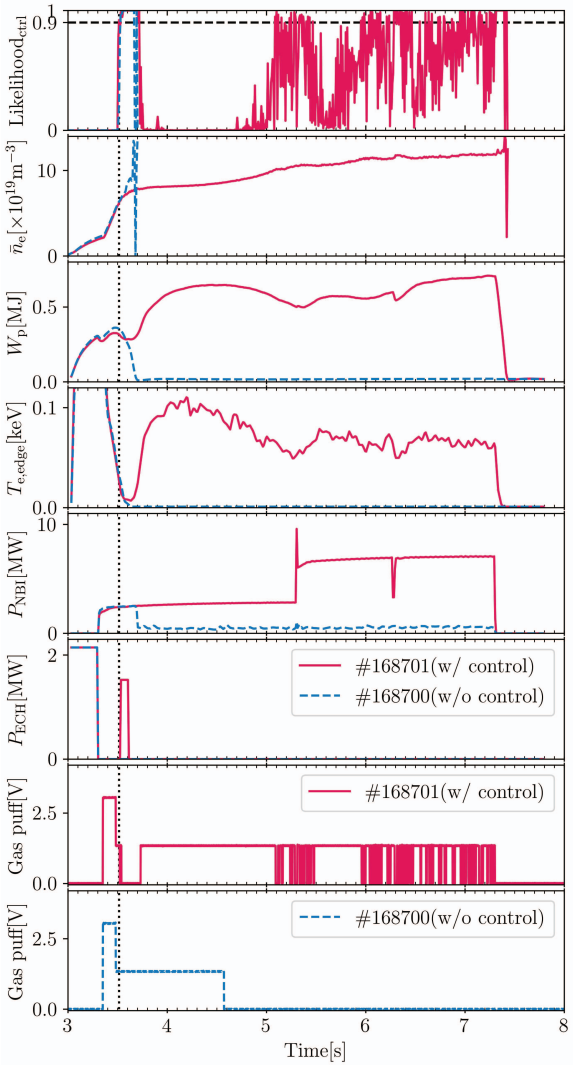

Fig. 2 The discharges with and without collapse avoidance control in hydrogen plasma, shown by red and blue lines, respectively. The dashed horizontal line in the top panel and the dotted vertical line show the threshold value and the time when the likelihood exceeded the threshold at first, respectively.

In the latter part of the discharge with control, the radiative collapse has been avoided only by turning on/off gas puff and $\bar{n}_e$ was developed above $1.2 \times 10^{20}\,\mathrm{m}^{-3}$. In this phase, the ECH was unavailable because of the technical limitation of duration time. When the change of NBI heating power occurred at around 5.3 s and 6.3 s, the predictor detected the occurrence of the radiative collapse, and the high-density plasma was successfully sustained by the control. When the collapses were avoided, the recoveries of electron temperature $T_{e,edge}$ and diamagnetic energy W_p were observed.

The oscillation of the control signal, i.e., the oscillation of the likelihood, is mainly caused by the oscillation of $T_{e,ECE}$ signal. Even a small oscillation is amplified by the strong dependence on $T_{e,ECE}$. It remains unclear how turning on/off of gas puff with intervals shorter than the confinement time scale of about 100 ms affects avoiding collapse.

3.2 Discussions on collapse avoidance

Radiative collapse is likely to occur when $\bar{n}_e$ is high; thus, reducing $\bar{n}_e$ is one possible way to avoid radiative collapse. However, the likelihood recovery was not accompanied by the decrease in $\bar{n}_e$, as shown in Fig. 2. This is also seen in Fig. 3, indicating the trajectory of the discharges with and without control on the contour of the collapse

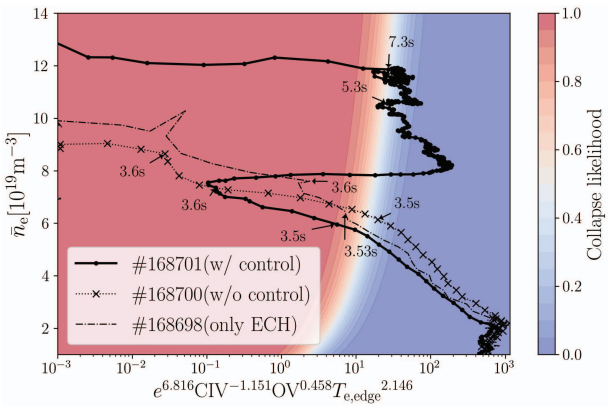

Fig. 3 The trajectory of the discharges (solid) with control, (dotted) without control, and (chain) with only ECH control on the color contour which shows the likelihood of radiative collapse against line averaged density and other extracted parameters.

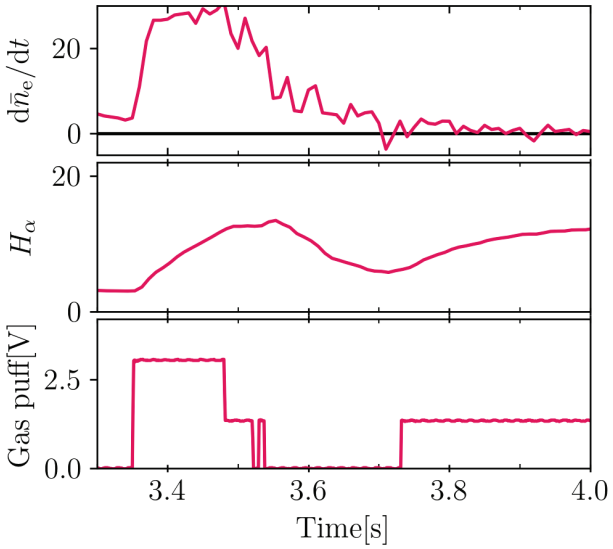

Fig. 4 The temporal changes of $\bar{n}_e$, H_α line emission, and the voltage signal that controls the gas puff in the discharge with collapse avoidance control system (#168701).

likelihood against line averaged density and the term of other extracted parameters. The likelihood shown in Fig. 3 is calculated with $T_{e,edge}$ and different from the likelihood used in the real-time control. In the discharge without control, shown by the dotted line in Fig. 3, once plasma entered the unstable (red) region, plasma went toward collapse.

In the discharge with control, it is seen that the plasma returns from the unstable (red) region to the stable (blue) region by the control, as shown in the solid line. Figure 4 shows that $\bar{n}_e$ kept increasing ($d\bar{n}_e/dt > 0$), even while the gas-puff fueling was turned off. During this time, recycling was reduced but not extinguished, as shown by H_α line emission in Fig. 4. This suggests that the fuel was supplied by the recycling from the vessel wall when the plasma was returning to the stable region.

In the latter phase of the controlled discharge, the plasma stayed in the stable region near the boundary while increasing the density. After the heating stopped at around 7.3 s, the plasma went into the unstable region and terminated. This result shows that regulating gas-puff fueling is effective in keeping plasma in the stable region. It also demonstrates that the control system can achieve a higher plasma density.

In other discharges with hydrogen plasma, collapse avoidance with only boost ECH has been attempted. In these cases, the collapse in the early phase has not been avoided. The chain line in Fig. 3 shows a discharge where collapse avoidance with only boost ECH has been attempted. In this discharge, the boost ECH was injected at 3.53 s and stopped at 3.6 s by the interlock. As shown in Fig. 3, the plasma state never returned to the stable region in this discharge. The possibility of avoiding radiative collapse with only boost ECH by changing operational conditions, such as off-axis injection, is under investigation.

4. Conclusion

In this study, a real-time collapse avoidance control system has been developed based on the result of the data-driven approach on radiative collapse. Collapse likelihood has been quantified using the SVM trained with the plasma parameters selected by ES, which is one of the sparse modeling techniques. The control system calculates the collapse likelihood in real-time; it actuates gas puff and ECH for fueling and additional heating, respectively.

The control system has been applied to density ramp-up experiments in hydrogen plasma in LHD to show that the predictor based on the collapse likelihood has the capability to predict a radiative collapse in real-time. Consequently, the radiative collapse in the initial density ramp-up phase has been avoided, and the control system has maintained high-density plasma. This is the first case to control stellarator-heliotron plasma to avoid radiative collapse based on the machine-learning results.

The discharges, where the plasma was about to collapse but was avoided to collapse, are good examples that reveal the radiative collapse mechanism. Further investigation focusing on plasma behavior, when the collapse was avoided, is underway.

Acknowledgements

The authors are grateful to the LHD experiment group for the excellent support of this work. This work is supported by the National Institute for Fusion Science grant administrative budgets NIFS21KLPP068, and JSPS KAKENHI Grant Numbers 17H01368, 19J20641, and 20K20426.

[1] S. Sudo *et al.*, Nucl. Fusion **30**(1), 11 (1990).
[2] A. Murari *et al.*, Nucl. Fusion **60**(5), 056003 (2020).
[3] C. Rea *et al.*, Fusion Sci. Technol. **76**(8), 912 (2020).
[4] K.J. Montes *et al.*, Nucl. Fusion **61**(2), 026022 (2021).
[5] J. Kates-Harbeck, A. Svyatkovskiy and W. Tang, Nature **568**(7753), 526 (2019).
[6] C. Rea *et al.*, Nucl. Fusion **59**(9), 096016 (2019).
[7] W. Hu *et al*. Nucl. Fusion **61**(6), 066034 (2021).
[8] T. Yokoyama *et al.*, J. Fusion Energy **39**(6), 500 (2020).
[9] T. Yokoyama *et al.*, Plasma Fusion Res. **16**, 2402010 (2021).
[10] A. Iiyoshi *et al.*, Nucl. Fusion **39**(9Y), 1245 (1999).
[11] C. Cortes and V. Vapnik, Machine Learning **20**(3), 273 (1995).
[12] Y. Igarashi *et al.*, J. Phys.: Conf. Series **699**(1), 012001 (2016).
[13] C. Van Rijsbergen, *Information Retrieval*. (Butterworths, London, 1979).
[14] Y. Igarashi *et al.*, J. Phys.: Conf. Series **1036**, 012001 (2018).
[15] J. Miyazawa, K. Yasui and H. Yamada, Fusion Eng. Des. **83**(2), 265 (2008). Proceedings of the 6th IAEA Technical Meeting on Control, Data Acquisition, and Remote Participation for Fusion Research.
[16] T.I. Tsujimura *et al.*, Fusion Eng. Des. **153**, 111480 (2020).
[17] T.I. Tsujimura *et al.*, Nucl. Fusion **61**(2), 026012 (2021).